

# Silicon LEDs in FinFET technology

G. Piccolo<sup>1</sup>, P.I. Kuindersma<sup>3</sup>, L-A. Ragnarsson<sup>2</sup>, R.J.E. Hueting<sup>1</sup>, N. Collaert<sup>2</sup>, and J. Schmitz<sup>1,\*</sup>

<sup>1</sup>MESA+ Institute for Nanotechnology, University of Twente, Enschede, The Netherlands

<sup>2</sup>imec, Leuven, Belgium.

<sup>3</sup>NXP Semiconductors (now at Eindhoven University of Technology), Eindhoven, Netherlands

\*j.schmitz@utwente.nl

**Abstract**—We present what to our best knowledge is the first forward operating silicon light-emitting diode (LED) in fin-FET technology. The results show near-infrared (NIR) emission around 1100 nm caused by band-to-band light emission in the silicon which is uniformly distributed across the lowly doped active light-emitting area. We also propose further improvements to exploit the full potential of this structure.

**Index Terms**—Silicon, Silicon on insulator technology, Electroluminescence, Elemental semiconductors, Light emitting diodes, p-i-n diodes, FinFETs, LED, Carrier injectors, Integrated optics, Near-infrared light emission, Infrared light sources, Silicon Photonics, Nanometric devices.

## I. INTRODUCTION

Efficient light emission from silicon-based devices has been presented as one of the holy grails in electrical engineering [1]. The literature reports on a wide range of potential candidate light emitters that may be integrated with microelectronics. Most effort is spent on integrating optical active material on silicon, that is mainly used as passive carrier. For a review of these, see e.g. [2], [3]. If we consider the criteria to target a successful integration in state-of-the-art VLSI platforms, i.e. a full compliance to CMOS fabrication standards and an operative voltage conform to the supply range of modern chips (or even better suitable for low power applications), many of the approaches reported in [2], [3] are not optimal. Band-edge emission from silicon, instead, can be stimulated at low power with relatively simple device architectures: therefore we present a silicon LED based on a forward-biased p-i-n diode structure.

The choice of silicon as an active (light-emitting) material is less intuitive. The radiative lifetime for electron-hole recombination in silicon is relatively long compared to non-radiative lifetimes, and therefore the probability of non-radiative recombination is higher. Shockley-Read-Hall (SRH) recombination will dominate at low carrier injection levels, while Auger recombination at high injection (above  $\sim 10^{18}$  carriers per  $\text{cm}^{-3}$ ). Proper tuning of the injection level, combined with high quality material to limit SRH, allows to benefit from the relatively low surface recombination of the interface silicon-thermal oxide, resulting in a potentially sufficient efficiency. Several groups [4], [5] have been predicting a theoretical maximum of 20 % internal efficiency for silicon LEDs. In practice, the efficiency record, to the best of our knowledge, was achieved by Green et al. [6] with a reported 0.92% external quantum efficiency on forward-biased silicon LEDs.

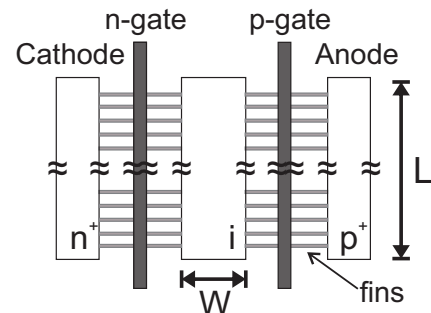


Fig. 1. Schematic topview of the LED. The device is a p-i-n diode with an intrinsic (active) region of  $L \times W$ . The intrinsic region is connected to the extensions via a series of gated fins, whose number depends on the actual dimensions of the device (dimensions and pitch of the fins are fixed). The actual junction on each side falls beneath the gate. The figure is not to scale.

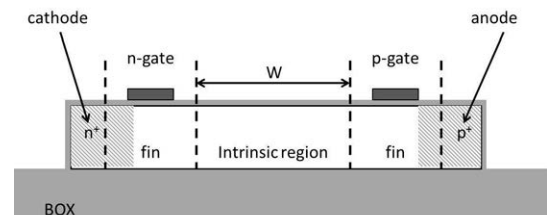


Fig. 2. Schematic cross-section of the LED in the sense of the current, along one fin. The device is a p-i-n diode gates at the two junction sides. The dashed lines delimit the fin region. The figure is not to scale.

Yet, the LED presented by Green et al. has an active (light emitting) volume in the order of  $\text{mm}^3$ , whereas much higher granularity is necessary both to reduce costs and maximize the out-coupling of the light in integrated waveguides. Compact, efficient LEDs has been previously fabricated on silicon-on-insulator (SOI) with an active volume of  $24 \mu\text{m}^3$  [7]. In such miniaturized configurations, surface recombination and carrier injector design come into play, as demonstrated in recent work from our group, where studies of injector scaling [8], [9] indicate that a smaller injector may lead to better quantum efficiency. When scaling down to nano-injectors, it is imperative to ensure a smooth conduction (i.e. no interfaces in the current path) as well as to control properly the quality of the surfaces of the injectors, to limit surface recombination. To

accomplish that, in the current work we make use of finFET technology to form nanometer-dimensioned gated injectors for electrons and holes; at the same time, the active emitting region can be kept at a more favorable surface-to-volume ratio. Hoang et al. [7] proved the field effect to be an effective means to tune the injection through a junction. However, the effect is more prominent if field control is pushed to the extreme, as in a gate-all-around structure; hence the choice of fin injectors. This novel approach has the advantages of a standard fabrication process, better dimensional control and the possibility to optimize the intrinsic region width and the injector widths separately. To our knowledge, these are the first silicon LEDs realized in finFET technology.

## II. EXPERIMENTAL

All devices have been fabricated at imec in a standard finFET technology from high quality silicon-on-insulator substrates. The SOI layer is 65-nm thick on a buried oxide layer (BOX) of 145 nm.

The LEDs are p-i-n diodes with the junctions formed on gated silicon fins. See Fig. 1 for a topview of the device and Fig. 2 for the schematic of a cross-section taken along the direction of the current. The gates run over all fins on each junction side. The gate stack consists of 2.5 nm SiON/5 nm TiN covered with 100 nm polysilicon; the latter layer is doped together with the closer ( $p^+$ ,  $n^+$ ) extension region ( $5 \cdot 10^{19} \text{ cm}^{-3}$ ). The fins are 240-nm long and 10-nm wide, with a fixed pitch of 200 nm; the number of fins scales with the length of the device  $L$  (i.e. the fins cover the whole length of the intrinsic region). The length of both gates is 60-nm and they are situated at the center of the fins.

The p-side of the diode is referred to as the anode, the n-side as the cathode.

We had available a variety of devices with different lengths ( $L$ ) and widths ( $W$ ) of the intrinsic region. The latter is the volume where light generation is expected to be more efficient, because of the favorable surface-to-volume ratio. All results that follow, unless stated otherwise, are relative to a reference device with  $L = 62 \mu\text{m}$ ,  $W = 8 \mu\text{m}$  ( $L$  and  $W$  as defined in Fig. 1).

All devices have been characterized at room temperature on wafer level on a Karl Süss probe station. Electrical characterization has been carried out with a Keithley 4200 Semiconductor Characterization System. Light emission has been recorded via the microscope with infra-red (IR) objective lenses with a Xenics camera, featuring a cooled InGaAs sensor of  $256 \times 320$  photodiodes; the range of detection of the camera is in the near infra-red (NIR), from 900 to 1700 nm. The camera can be extended with a Specim Inspector spectrometer for spectral measurements.

## III. ELECTRICAL BEHAVIOR

When both gates are grounded we observe rectifying operation, exhibiting current-voltage ( $I-V$ ) characteristics with an ideality factor of about 1.6. An example is given in Fig. 3. The non-ideality is attributed to the high recombination probability

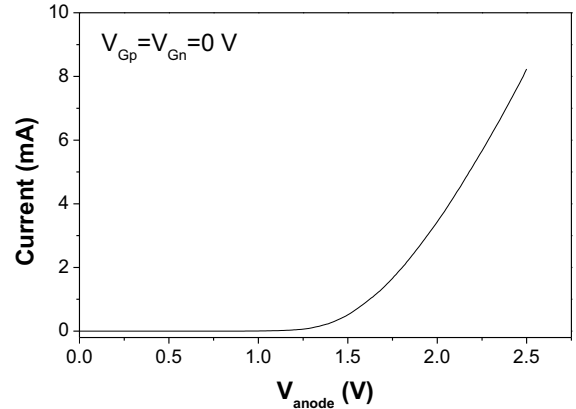


Fig. 3. Current-voltage plot for a device with an intrinsic region of  $L = 62 \mu\text{m}$ ,  $W = 8 \mu\text{m}$  ( $L$  and  $W$  as defined in Fig. 1). Both gates are grounded in this example.

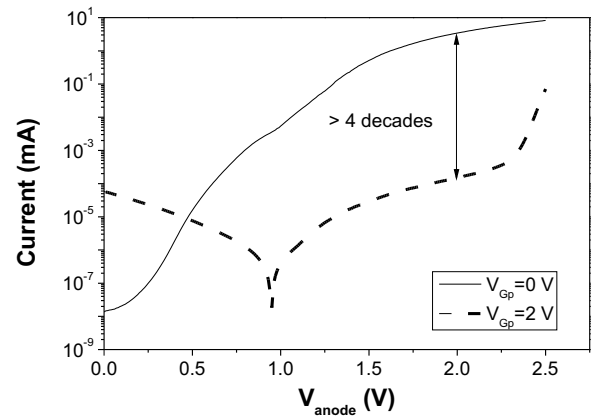


Fig. 4. Example of gate control. The plot reports the semi-logarithmic  $I-V$  characteristics for a p-gate bias of 0 V (same as in Fig. 3) and 2 V. In both cases the other gate (n-gate) and cathode are grounded. Applying a positive voltage to the p-gate reduces the current in the high-injection regime of more than four orders of magnitude.

in the fins. Similarly, the change of slope which can be observed around 1 V in the semi-logarithmic plot (solid line in Fig. 4) could be ascribed to the intrinsic part of the fins. Design rules prohibited the layout of gates fully covering the fin's length: as a consequence, this geometry has not yet been optimized for conduction nor for light emission efficiency.

The two gates have the potential to act as valves for the injection of holes (p-side) and electrons (n-side). Moreover, when appropriately biased, the two gates can create a barrier for carriers to diffuse towards the opposite electrode (see [7] for further details); hence this structure has the potential to limit injection and therefore Auger recombination. The diode current is high only when both electron and hole injection are significant, as in the intrinsic region current is sustained by recombination [10], [11]. This means that switching the gates, the current could be suppressed, as demonstrated in Fig. 4. In principle, this offers the possibility of fast switching of the light emission. Yet, the control of the gates in the present devices is irregular; a proper control from the gates requires further study and an optimization of the design by a more

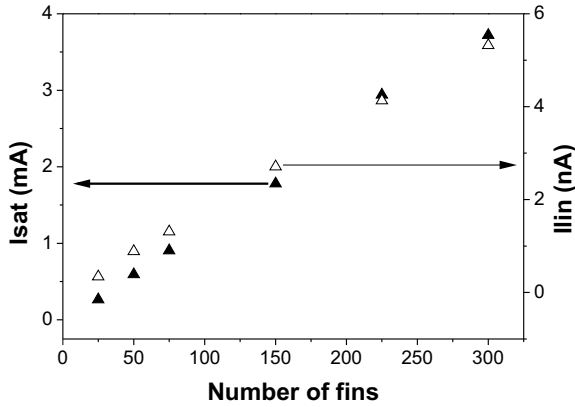


Fig. 5. Saturation (left axis, filled symbols) and linear (right axis, empty symbols) currents plotted against the number of fins (i.e. the length of the intrinsic region  $L$ ). The saturation current is sampled at a forward bias of 2 V where the device is in high injection regime, while linear current at 0.3 V (low injection). In both cases both gates are grounded.

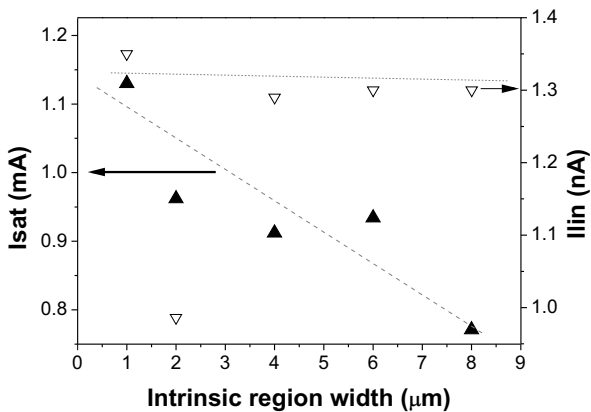


Fig. 6. Saturation (left axis, filled symbols) and linear (right axis, empty symbols) currents plotted against the width of the intrinsic region  $W$ . The saturation current is sampled at a forward bias of 2 V where the device is in high injection regime, while linear current at 0.3 V (low injection). In both cases both gates are grounded. For both currents, a general trend line is indicated, to guide the eye.

detailed modeling of the fin regions.

In the current design, the conduction is mainly determined by the fins. Indication of this behavior comes by observing the total current trends with the geometrical dimensions.

The dependency of both high- and low-injection currents on the number of fins, which is reported in Fig. 5, appears to be in agreement with the expected behavior for a normal p-i-n diode. The pitch of the fins is fixed to 200 nm, which means that the length of the intrinsic region  $L$  (see Fig. 1) increases proportionally with the number of fins. A longer intrinsic region offers a lower resistance (which affects the saturation current) and, since width and thickness are unchanged, gives a larger volume for recombination current (which affects the linear regime of the  $I - V$ ).

In order to distinguish the effect of the fins from that of the active region on the total current of the device the intrinsic region width  $W$ , as defined in Fig. 1, has been varied as

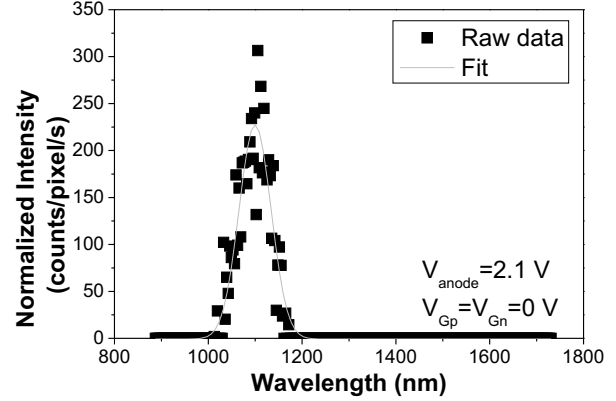


Fig. 7. Example of electro-luminescence (EL) intensity versus wavelength for the LED: the original data are shown in squares, while the gray line shows the fitted peak (gaussian) used for analysis. The spectrum shows a peak at about 1100 nm, with a FWHM of 80 nm, which is ascribed to near-band-edge emission from silicon. No signal could be detected below the wavelength of 900 nm.

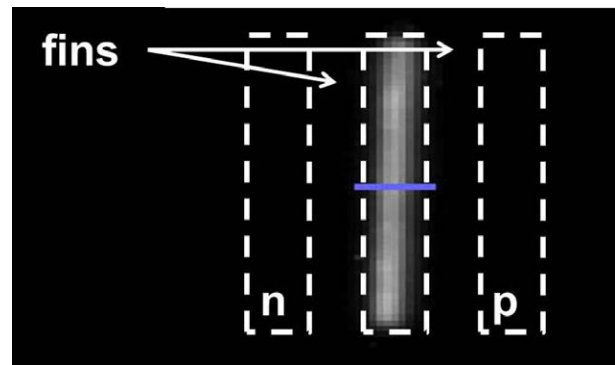


Fig. 8. NIR image of emission from the top surface of the LED. The dashed lines show the position of the three regions of the device. Light is emitted uniformly from the complete visible surface of the intrinsic region. No measurable emission is visible from the fins.

well. In Fig. 6 we see both high- and low-injection currents plotted against  $W$ . For the saturation current, extracted in high injection regime, we can observe a general decreasing trend, though the behavior is quite irregular. A decreasing trend is consistent with the increase in series resistance with  $W$ , but the irregularity of the plot indicates that there are concurring factors in determining the total current of the device. In addition, the linear current is almost independent on  $W$ , whereas in a normal p-i-n diode, where recombination is important, the current should increase with it [11]. In low injection regime, the recombination in the intrinsic region should be dominating the conduction, and therefore the current should increase with the volume (i.e. linearly with  $W$  in our case). Both behaviors of saturation and linear current indicate that conduction is determined less by the intrinsic region, as would happen in a normal p-i-n diode, but by the fins.

#### IV. LIGHT EMISSION

Fig. 7 shows the light emission properties of the device. The spectral peak is centered at a near-infrared (NIR) wavelength of about 1100 nm with a FWHM (full-width-half-maximum)

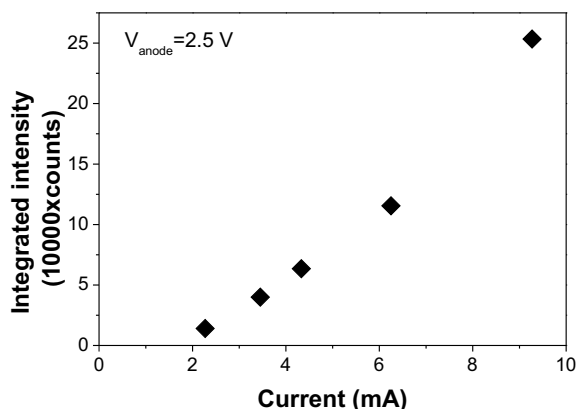


Fig. 9. Intensity-Current plot. In this case both gates are grounded and the bias is applied between anode and cathode.

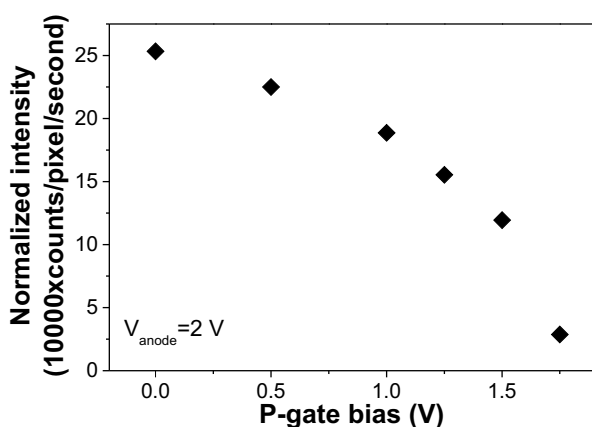


Fig. 10. Intensity per pixel area per second as a function of the positive voltage applied on the p-gate. This is an example of the potential gate control on light emission. In this case the p-gate is positively biased, while the diode is kept at a constant forward bias of 2 V. The other gate and the cathode are grounded. The diode operates in high-injection regime.

of 80 nm, showing the typical signature of band-to-band recombination in silicon [12]. The emission takes place in the intrinsic region and is uniform over its surface (see Fig. 8). No emission from the fins is observed neither in the spectrum or in the IR photo of the device.

Figure 9 shows the intensity-current  $L - I$  characteristic. Here, the light emission from the top surface of the device has been integrated over the spectrum and plotted against the current flowing in the device. The linear dependency indicates the absence of gain. It also suggests that by employing the gates action, the light could be switched on and off. We report evidence of the gate action through the current in Fig. 10, where the normalized intensity is reported with respect to the voltage applied on the (p-) gate. The effect of the gate bias is, as shown in Fig.4, to limit the current in the device. As a result, the emission also reduces. Our equipment does not allow any time resolved measurement, so we have not been able to confirm this potential light modulation in the time domain.

## V. CONCLUSION

We presented, to our best knowledge, the first forward operating silicon LED in finFET technology.

In this concept the injection of electrons and holes into a lowly doped silicon volume is controlled by gated fins. The device operates as a gated p-i-n diode where the fin regions limit the current and consequently the light output in the central emitting volume. The LED operates at low power and is fully compliant to state-of-the-art VLSI production lines.

The device shows near-infrared light emission, characterized by the distinctive spectral peak around 1100 nm of band-to-band from silicon. The emission is uniform across the lowly doped silicon volume. The gate potentials influence the current flow and therefore the light emission intensity, opening the possibility of fast switching.

Further work is required to enable a proper control of the gates and enhance the emission efficiency, in particular by reduction of the spacing between the intrinsic region and the access gates.

## ACKNOWLEDGMENT

The authors are thankful to Marc Aoulaiche from imec for providing the wafers. The authors gratefully acknowledge the support of the Smart Mix Programme of the Netherlands Ministry of Economic Affairs and the Netherlands Ministry of Education, Culture and Science.

## REFERENCES

- [1] N. R. Savage, "Holy grail: Light from silicon," *IEEE Spectrum*, January 2004.
- [2] L. Pavesi, "Will silicon be the photonic material of the third millennium?" *J. Phys. Cond. Matter*, vol. 15, no. 26, pp. 1169–1196, 2003.
- [3] B. Jalali and S. Fathpour, "Silicon photonics," *Lightwave Technology, Journal of*, vol. 24, no. 12, pp. 4600–4615, 2006.
- [4] T. Trupke, J. Zhao, A. Wang, R. Corkish, and M. A. Green, "Very efficient light emission from bulk crystalline silicon," *Applied Physics Letters*, vol. 82, no. 18, pp. 2996–2998, 2003.
- [5] M. Kittler, M. Reiche, T. Arguirov, W. Seifert, and X. Yu, "Silicon-based light emitters," *physica status solidi (a)*, vol. 203, no. 4, pp. 802–809, 2006. [Online]. Available: <http://dx.doi.org/10.1002/pssa.200564518>
- [6] M. Green, J. Zhao, A. Wang, P. Reece, and M. Gal, "Efficient silicon light-emitting diodes," *Nature*, vol. 412, pp. 805–808, 2001.
- [7] T. Hoang, P. LeMinh, J. Holleman, and J. Schmitz, "Strong efficiency improvement of SOI-LEDs through carrier confinement," *IEEE Elect. Dev. Lett.*, vol. 28, pp. 383–385, 2007.
- [8] V. Puliyankot, G. Piccolo, R. J. E. Huetting, A. Heringa, A. Kovalgin, and J. Schmitz, "Increased light emission by geometrical changes in si leds," in *Group IV Photonics (GFP), 2011 8th IEEE International Conference on*, 2011, pp. 287–289.
- [9] G. Piccolo, A. Y. Kovalgin, and J. Schmitz, "Nanoscale carrier injectors for high luminescence si-based leds," *Solid-state electronics*, vol. 74, pp. 43–48, April 2012.
- [10] S. Sze, *Semiconductor Devices*, 3rd ed. John Wiley & Sons, 2007.
- [11] V. Puliyankot and R. J. E. Huetting, "One-Dimensional Physical Model to Predict the Internal Quantum Efficiency of Si-Based LEDs," *IEEE Trans. Electron Devices*, vol. 59, no. 1, pp. 26–34, January 2012.
- [12] H. Schlagenotto, H. Maeder, and W. Gerlach, "Temperature dependence of the radiative recombination coefficient in silicon," *physica status solidi (a)*, vol. 21, no. 1, pp. 357–367, 1974. [Online]. Available: <http://dx.doi.org/10.1002/pssa.2210210140>